New Oblate Bands in Light-Lead Nuclei

R. M. Diamond
Nuclear Science Division, Lawrence Berkeley Laboratory, Berkeley, California 94720

A number of rotational bands have been found in light-lead nuclei. But the transitions between the states are predominantly of M1 multipolarity rather than E2. In at least one case where the lifetimes were measured, the values of B(M1) found were among the largest known, while the values of B(E2) for two crossover transitions are relatively small, of order 15 single-particle units. These bands also show other interesting properties, and the connecting transitions to the lower bands in the nucleus have usually not been found.

After the discovery of superdeformed (SD) bands in nuclei near A=192 [1-3], the continuing search for additional SD bands and the investigations of their unusual properties has provided very extensive $\gamma\gamma$ coincidence data for a number of nuclei in that region. These data allow a much more detailed investigation of the more normally deformed bands than ever achieved in the past. And this is an interesting region to study because of the possibilities for the co-existence of different shapes. For example, the semi-magic, neutron-deficient lead isotopes near ^{208}Pb have long been studied as examples of single-particle and few-particle excitations. But calculations for more neutron-deficient Pb isotopes indicate that prolate and oblate, as well as superdeformed, minima are possible [4-6]. The former involve the high-j proton $i_{13/2}$ and $h_{9/2}$ and neutron $i_{13/2}$ orbitals. These, particularly the protons, are shape-determining orbitals in this region. In addition, the question arises whether at higher excitation and spin the multiparticle excitations can lead to a form of collective behavior. The answer appears to be a qualified yes, and is exemplified by a new type of band in this region which I would like to discuss with you.

Let me start by showing Fig. 1, which illustrates some of the first rotational bands of this type observed in lead nuclei; these are bands in ^{199,200}Pb found by ref. [7]. They are typical of the "regular" bands found in $^{196\text{-}201}$Pb, and appear to be as good-looking rotational bands as deformed bands in the rare-earth region. However they are not stretched electric quadrupole (E2) transitions, but rather stretched dipole transitions, and most likely magnetic ones (M1). The stretched dipole nature is indicated in several cases by angular correlation and distribution measurements and by the E2 crossover transitions where observed. The magnetic character is suggested by the branching decay in competition with the E2 crossovers and by the large conversion electron coefficients required by the low-energy lines at the bottom of the bands in order to keep the intensity constant, as there is usually no evidence of gradual decay out of the band. The decay schemes for these bands [7] are shown in Fig. 2. The sudden transfer out of the band is a feature they share with the superdeformed ones, and another shared property is that until just recently the transitions connecting with the lower, yrast bands have not been found for either the SD or the new oblate bands. However, Prof. H. Hübel has informed me [8] that his group has found several more bands of this type in ^{199}Pb, and that for one of them connecting transitions to lower bands were found. In addition, two more bands have been found in ^{201}Pb [9].

At the same time that ref. [7] appeared, in fact in the same journal, an English-French

collaboration published [10] on a similar band in ^{198}Pb, and later [11] on two more in ^{197}Pb. Our Lawrence Livermore National Laboratory (LLNL)-Lawrence Berkeley Laboratory (LBL) collaboration observed [12] two such bands in ^{198}Pb (one the same as that described in [10]) and two more [13] in ^{197}Pb (again the stronger one, ≈ 10% of the isotopic intensity, is the same as that seen in [11]). Figure 3 shows a partial decay scheme for the two bands we observed in ^{198}Pb; it illustrates some of the features of these bands.

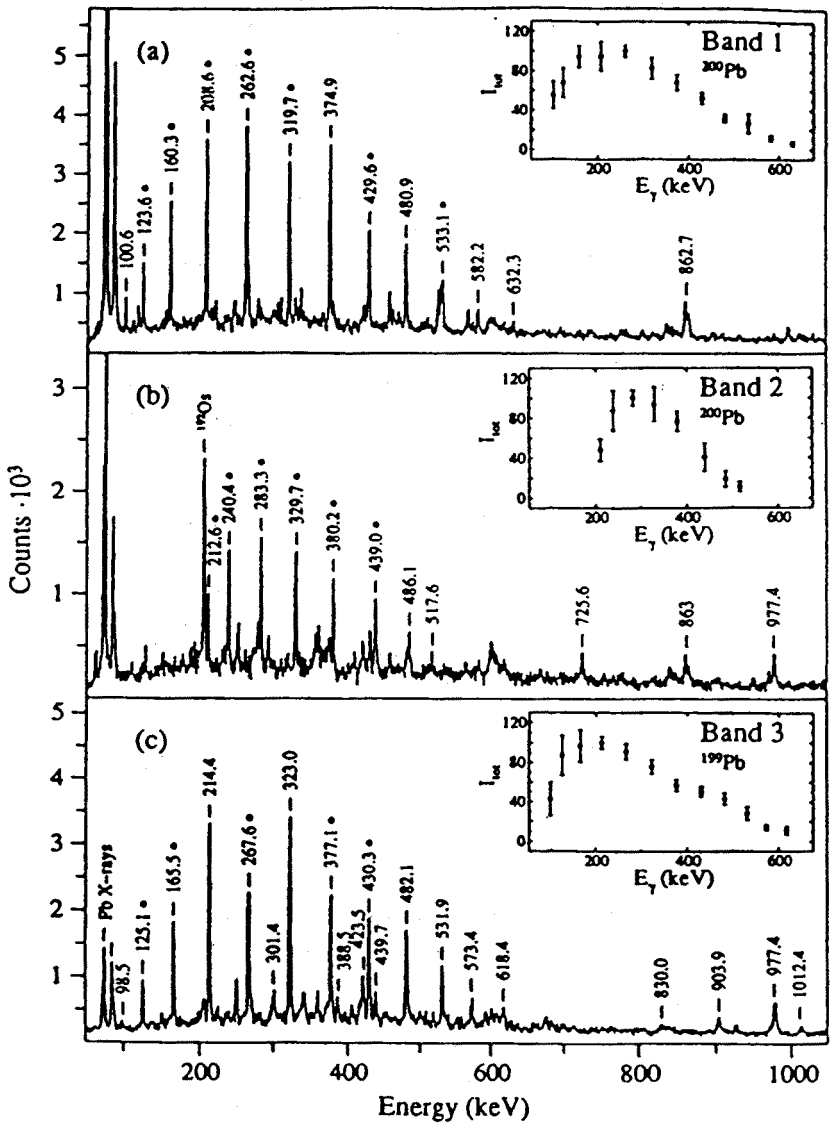

Fig. 1. Summed γ-ray coincidence spectra from gates on transitions marked by dots. (The 977-keV transition in spectrum (b) is from a contamination in two of the gates.) Figure is taken from Ref. [7].

Both thin, unbacked and Au- and Pb-backed targets were used in the ^{154}Sm (^{48}Ca, 4n) ^{198}Pb reaction at 205 MeV. A comparison of the relative intensities of transitions when using the backed and unbacked foils permitted finding isomers, as with the thin targets even a delay of a few nanoseconds would carry the compound-nuclear recoils out of the view of the (BGO-collimated) Ge detectors, while with the backings the isomer would be stopped in the target and observed, if its mean life was not much longer than the coincidence interval of the electronics. For example, the 228- and 306-keV transitions below band II and the lines below them are relatively stronger with the backed targets, indicating an isomeric state above them, and this is also true for the 630- and 930-keV lines in coincidence with the 322-keV transition below band I, and with the 541-keV line in coincidence with the 207- and 177-keV transitions and the lines above them. Even with the backed targets, nothing is seen

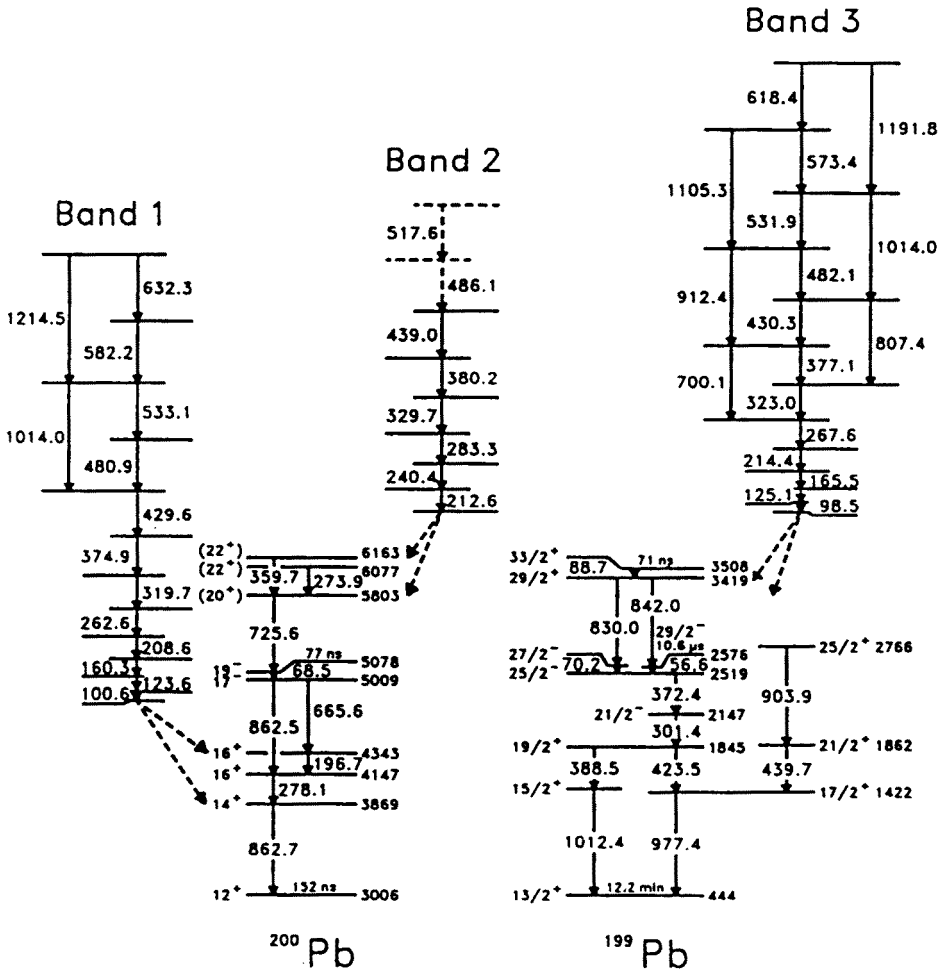

Fig. 2. Level schemes for the three rotational bands in $^{199,200}Pb$ shown in Fig. 1. Taken from Ref. [7].

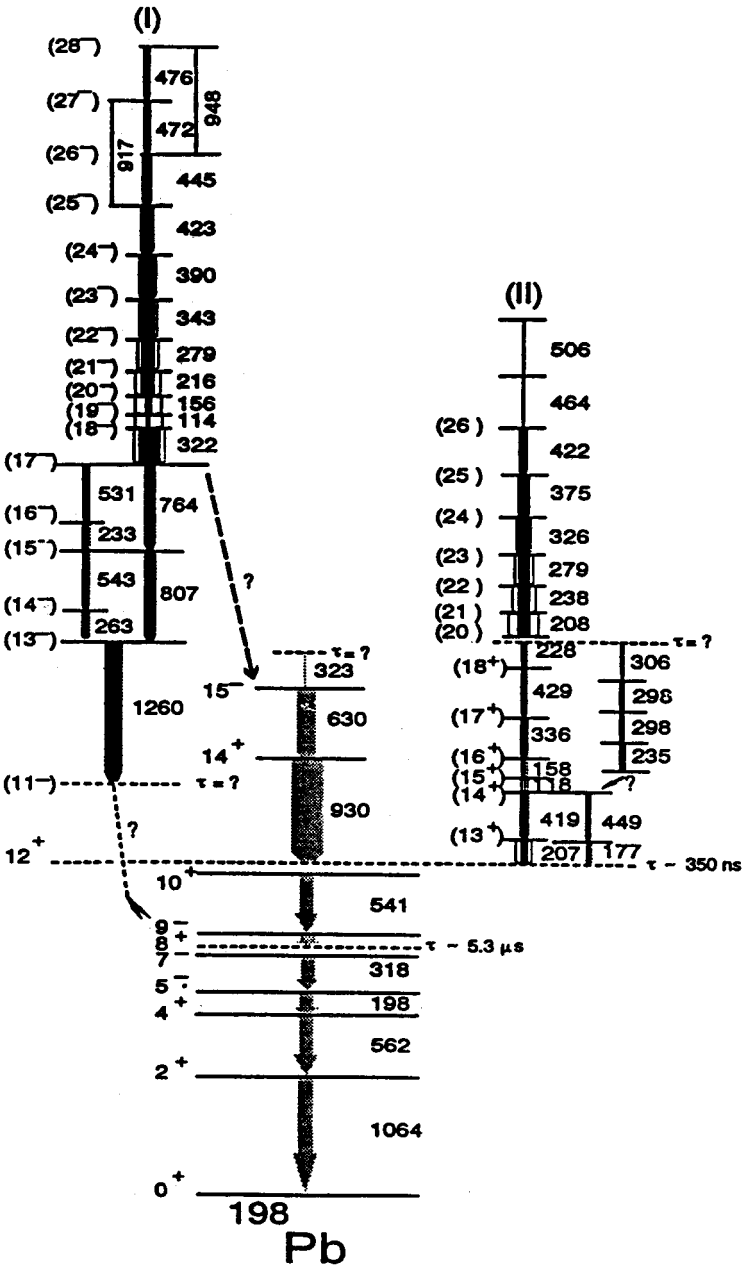

Fig. 3. Partial level scheme of ^{198}Pb. Previously known levels are in light gray, new low-lying levels in dark gray, and new bands are in black. Dashed lines represent suggested locations of isomeric states. Intensities of new transitions above the known 12^+ isomer are based on thin-target measurements (see text). Outer width of M1 transition arrows represents corrections for internal conversion (assuming pure M1 lines). Intensities below the 12^+ isomer cannot be determined accurately in this experiment. Taken from Ref. [13].

in coincidence with the strong line of 1260 keV, suggesting a long lifetime after it. There are three isomeric states seen systematically in the light Pb isotopes: two-proton 8^+ and 11^- states and a two-neutron 12^+ one. The 11^- state has not been found yet in ^{198}Pb, but it might be the state reached by the 1260-keV line, and if it decayed to the known 12^+ isomer that could explain why we see nothing connected to it even with the backed targets. But we do not know the spins of all the new levels observed; since no connecting transitions to the ground band were identified, the spins are only estimates, good perhaps to about $\pm 2\hbar$. When there are no cross-over transitions or parallel cascades to fix the order of the transitions, they have been arranged in order of increasing intensity, which is probably O.K. for the two bands but may not be true in general and leaves the order of the cascades below the two bands in some doubt.

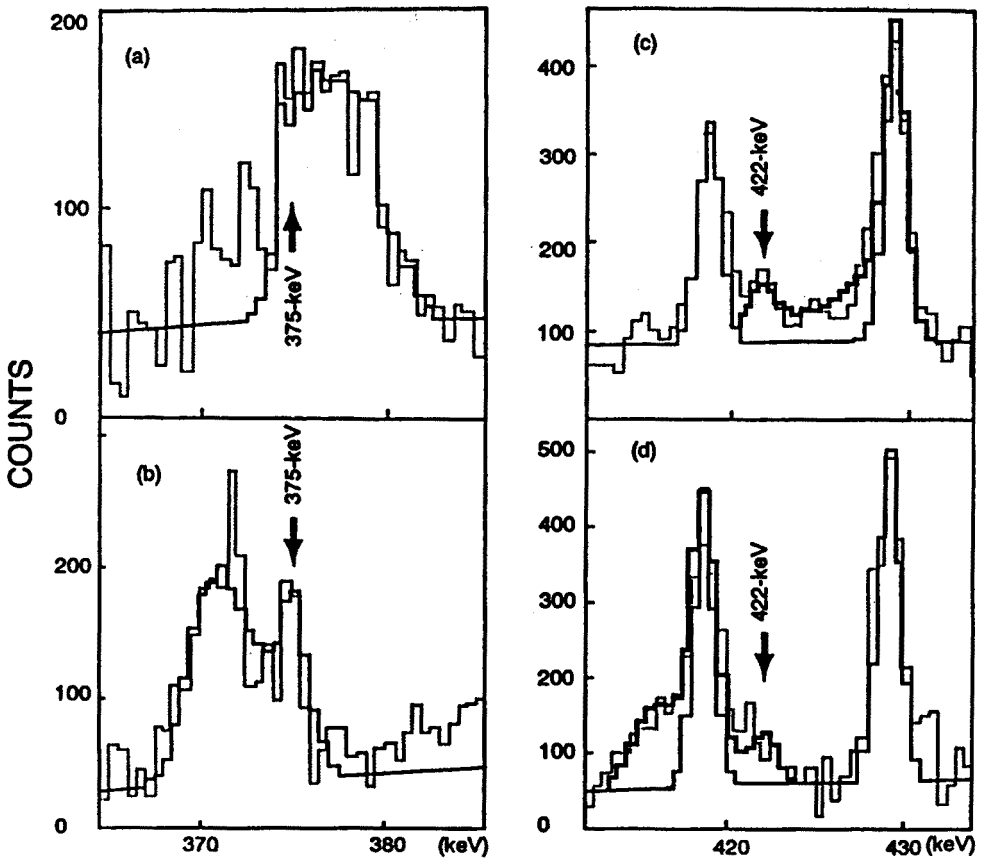

Fig. 4. Examples of DSAM fits in band II with Pb-backed target. Data are shown in light lines, fits with heavy lines. Forward, (a), and backward,(b), spectra of the 375-keV transition; stopped position shown by arrow. Forward, (c), and backward, (d), spectra for the 422-keV transition; stopped contaminant peaks at 419 and 429 keV are shown also. Taken from Ref. [12].

Directional correlation data indicated that the band members and most of the cascades below them consist of stretched dipole transitions with little quadrupole mixing, and intensity considerations of the low-energy members again suggested that only large M1 conversion electron coefficients would give nearly constant or increasing intensities, as shown in Fig.3. The two E2 cross-overs seen at the top of band I also indicate that the bands consist primarily of stretched M1's.

For these two bands, lifetimes were determined by the Doppler-shift attenuation method with both the gold- and lead-backed targets; the first measurement on this type of band. Lineshape analysis was performed for a half-dozen peaks in each band by fitting simultaneously the forward, backward, and ≈ 90° detectors with a Monte-Carlo based code [14]. The nuclear and electronic stopping powers were taken from the compilation by Ziegler et al. [15], and 5000 slowing-down histories were run for each backing with a time step of 0.002 ps. These were sorted according to the geometry of each group of detectors, and the lineshapes calculated from a solution of the cascade decay sequence by Bateman-type equations. The detector efficiencies, the transition energies, the experimental

		Pb-BACKING					Au-BACKING				
	E_γ (keV)	τ (ps)	B(M1) (W.u.)		B(E2) (W.u.)		τ (ps)	B(M1) (W.u.)		B(E2) (W.u.)	
BAND (I)	343	1.12(39)	0.53	$^{+0.29}_{-0.14}$			1.15(24)	0.52	$^{+0.14}_{-0.09}$		
	390	0.64(15)	0.67	$^{+0.20}_{-0.12}$			0.79(14)	0.55	$^{+0.12}_{-0.08}$		
	423	0.41(16)	0.85	$^{+0.54}_{-0.24}$			0.50(11)	0.70	$^{+0.20}_{-0.13}$		
	445	0.19(7)	1.6	$^{+0.9}_{-0.4}$			0.29(4)	1.1	$^{+0.2}_{-0.1}$		
	472	0.29(10)	0.72	$^{+0.65}_{-0.23}$			0.15(5)	1.3	$^{+1.0}_{-0.4}$		
	917				11.3	$^{+10.3}_{-3.6}$				20.6	$^{+15.9}_{-6.3}$
	476	0.31(11)	0.67	$^{+0.54}_{-0.21}$			0.23(7)	0.9	$^{+0.7}_{-0.3}$		
	948				9.7	$^{+7.9}_{-3.1}$				13.3	$^{+10.2}_{-4.4}$
BAND (II)	326	0.60(19)	1.1	$^{+0.5}_{-0.3}$			0.55(22)	1.2	$^{+0.8}_{-0.4}$		
	375	0.31(9)	1.6	$^{+0.6}_{-0.4}$			0.40(17)	1.2	$^{+0.8}_{-0.3}$		
	422	0.18(5)	2.0	$^{+0.8}_{-0.4}$			0.22(7)	1.6	$^{+0.7}_{-0.4}$		
	464	0.068(18)	4.0	$^{+1.5}_{-0.9}$			0.129(47)	2.1	$^{+1.2}_{-0.6}$		
	506	0.050(14)	4.4	$^{+1.7}_{-1.0}$			0.054(17)	4.0	$^{+2.0}_{-1.0}$		

Fig. 5. Results from the DSAM fits to bands I and II in ^{198}Pb from both Pb- and Au-backed targets. τ is the state lifetime (and must be corrected for electron conversion to obtain the reduced transition probability). W.u. stands for Weisskopf single-particle unit. Taken from Ref. [12].

side-feeding intensity for each state in the band (with each side-feeding cascade assumed to consist of as many transitions as the main cascade up to five, and with the same transition energies but a single independent reduced-transition probability), and a number of rotational transitions above the highest transition observed were taken into account. Examples of the calculated fits and of the experimental lineshapes are shown in Fig. 4. Best fits were obtained with lifetimes of the side-feeding transitions somewhat longer than those of the cascade members.

The statistics are not great, so the errors are relatively large, but the lifetimes obtained from the two backings (which differ in stopping times by a factor of two) are shown in Fig. 5. They are in agreement, usually by ≈ 25% (although in the worst two cases it is a factor of two). The M1 lifetimes (in picoseconds) can be changed into B(M1)'s using the transition energies (in MeV) and branching ratios, where known, by means of the expression

$$B(M1; I \rightarrow I\text{-}1) = 0.0562 / \tau_{M1} (E_\gamma)^3 \quad \text{in } [\mu_N^2] \qquad (1)$$

These range in the present case from 0.9-2.7 μ_N^2 (0.5-1.5 Weisskopf units) for band I and from 1.8-7.2 μ_N^2 (1-4 W.u.) for band II. The latter are among the strongest B(M1)'s observed in masses greater than 90, and even those of band I are very strong [16]. The right order of magnitude is given by the formula of Donau and Frauendorf [17], but the variation with spin is different; either something is left out of the model, or something is changing in the real nucleus that we have not considered. Where two crossover E2 transitions were seen in band I and the branching ratios determined, B(E2) values could also be calculated from

$$B(E2; I \rightarrow I\text{-}2) = 0.08176 / \tau_{E2} (E_\gamma)^5 \quad \text{in } [e^2b^2] \qquad (2)$$

They are 0.068-0.136 e^2b^2 (10-20 W.u.); not large, but not small either, giving $Q_0 \approx 2b$. From not seeing E2 crossover transitions at the top of band II, we can estimate an upper limit there of <3 b. These values lead to a $\beta_2 < 0.1$. This is less than the oblate deformation suggested by theoretical calculations (see below), but it has two sources of error, the lifetime determinations and the branching ratios, as well as making use of the rotational model and formulae to go from the B(E2) to the value of Q_0 and then to the β_2. However, it seems unlikely that the average value of B(E2) obtained, 15 W.u., is off by as much as a factor of two larger, as then the two values of the branching ratios observed, λ = Intensity(ΔI=2) / Intensity(Δ=1) = 0.27 and 0.22, would most likely have to be two times larger. This, in turn, would make the ratio of B(M1)/B(E2), calculated via the expression

$$B(M1)/B(E2) = 0.697\, E(\Delta I=2)^5 / E(\Delta I=1)^3 \lambda(1+\delta^2) \quad \text{in } [\mu^2/e^2b^2] \qquad (3)$$

(where δ^2 is the mixing ratio, of order 1% in the present case, and the transition energies are in Mev) a factor of two smaller than the values of 16 and 22 actually obtained. But these bands in the neighboring nuclei do have values of 20-25, not 10. So the results of the lifetime measurements leave us with two surprises: the M1 transitions appear extraordinarily strong, but dipole moments do not lead to collective bands in the usual sense of quadrupole deformation (or octupole deformation), and the E2 transitions are weak

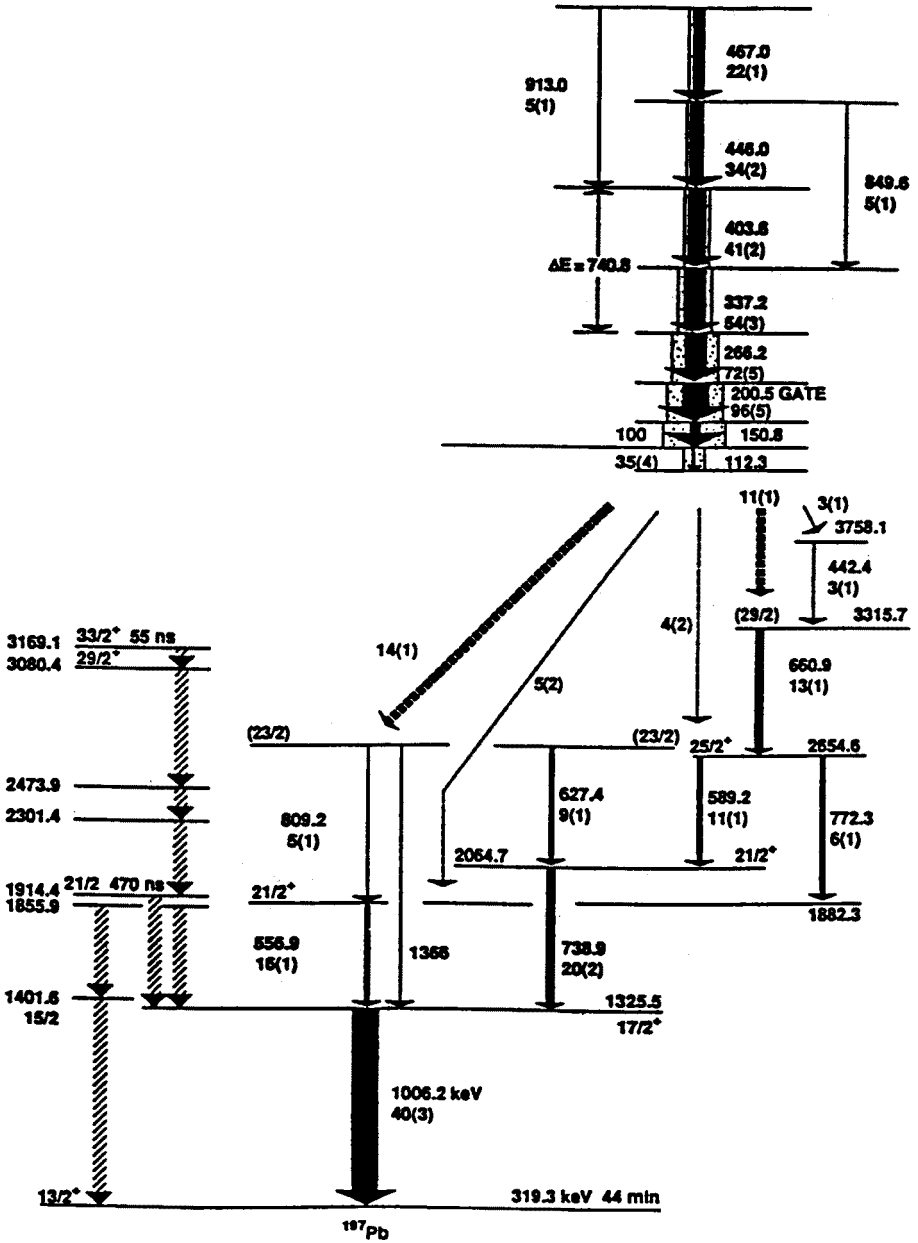

Fig. 6. Partial level scheme of regular band and its coincident transitions in ^{197}Pb. The width of the black arrows is proportional to the γ-ray intensity; the full width includes internal conversion (assuming pure M1 transitions). Intensities are obtained from a coincidence spectrum gated on the 200.5-keV transition. Taken from Ref. [13].

enough to make it hard to understand why the bands look so good with such regular spacing between the transitions.

Next we come to ^{197}Pb; here the LLNL-LBL group has seen two more regular bands, but also an irregular one [13]. A short note on two regular bands in this nucleus has been published by the English group [11], and the scheme for the stronger band seen by both groups is shown in Fig. 6. Again by comparing the intensities using multiple thin targets with those from a thick target, it was possible for us to determine that the decay of the state leading to the 112.3-keV line with ≈ 35% of the intensity of the previous transition goes mainly (>50%) to the $33/2^+$ isomeric state at 3169.1 keV. Since this state is considered to be the aligned neutron $(i_{13/2})^3$ state, its preferential feeding would seem to suggest that the rotational band also involves these three neutrons.

All of the regular bands have essentially the same properties as in the heavier nuclei, and these properties are summarized below.

1. Transition energies increase monotonically up the band; they look like a collective rotational band.
2. They consist mainly of M1 transitions; if crossover E2 transitions appear, they are only at the larger transition energies. B(M1)/B(E2) ratios are large, ranging from 15-45.
3. Values of δ, the mixing amplitude, are small (where determined from DCO ratios) and appear to be negative, indicating oblate deformation.
4. Intensities are difficult to determine because of isomers, but usually are of order 10% of the ground band, sometimes less.
5. Bands show little signature splitting, suggesting high-K, strong-coupled bands.
6. They have small values for the dynamic moment of inertia compared to the kinematic moment.
7. Until very recently, no transitions have been found connecting these bands to the lower-lying yrast bands that are in coincidence with them.

The irregular band in ^{197}Pb has many, but not all, of the properties of the regular bands and its decay scheme is shown in Fig.7. The transition energies are obviously irregular, but not completely irregular; the cascade is dominantly M1 transitions in the range of 120-400 keV, that is, a limited range of energies. There are some crossover E2 transitions that together with the M1's determine the order of the levels they encompass. And again no definite connections to lower states have been found yet, although a number of lower states are reached in the decay of the band. About 75% of the band intensity is found in the lower states, leaving about 25% lost in isomeric ones. Lifetime measurements have not been made on an irregular band yet, but one possibility to explain the irregular order is that they have smaller deformation and hence B(E2) values. Since in ^{197}Pb the B(M1)/B(E2) ratios for the irregular band (12-28) average about the same as the values for the regular band (20), the B(M1) values must also then be proportionally smaller, in that case at least.

Lastly, I show you the decay scheme, Fig. 8, worked out for an irregular band in ^{194}Pb by M. Brinkman [18]. This too was a floating band of predominantly M1 transitions, but with enough weak E2 cross-overs to determine the order. This band was first observed by B. Fant et al. [19], but because of poorer statistics they did not find the E2 crossovers (which are an order of magnitude weaker than the M1's) and so obtained a different and presumably incorrect order. Still more recently, F. Hannachi et al. have reported [20]

finding some of the connecting transitions between this band and lower states; as with the ^{199}Pb case, publication of these results should give the excitation energy and spin of the bandhead and thus help determine the nucleonic configurations involved.

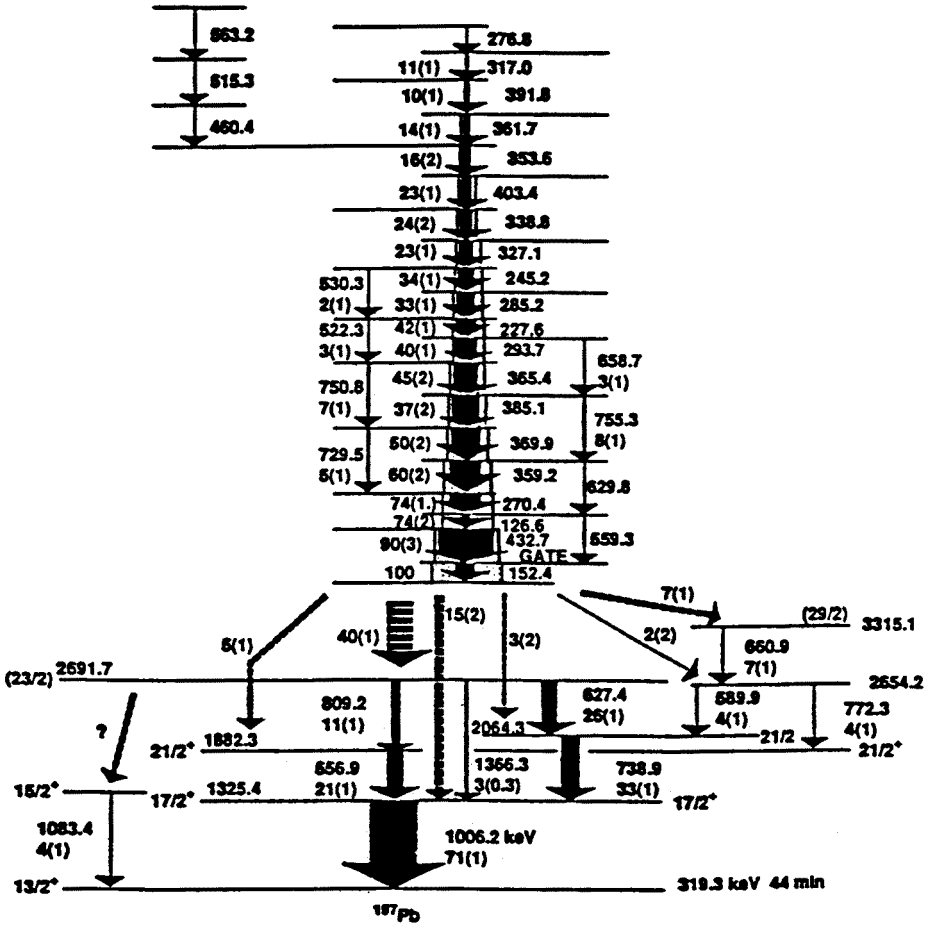

Fig. 7. Same as Fig 6, but for the irregular band in ^{197}Pb. Intensities are obtained from a coincidence spectrum gated on the 432.7-keV transition. Taken from Ref. [13].

So what is the nature of these bands? To be honest , the details are not yet known, but some features are clear, and it is fun to speculate a little. The existence of regular oblate bands has already been described in the mass-130 region, e.g., Fossan et al. [21] and references therein; the oblate driving force was ascribed to a combination of a lower-shell (high-Ω) $h_{11/2}$ proton and a pair of higher-shell (low-Ω) $h_{11/2}$ neutrons. The high-Ω proton provides a large positive g-factor and K value, yielding a large B(M1), which is further enhanced by the low-Ω $h_{11/2}$, as can be seen from the geometrical exposition of Donau and Frauendorf [17]. The E2/M1 mixing amplitude is small and its sign, which depends upon

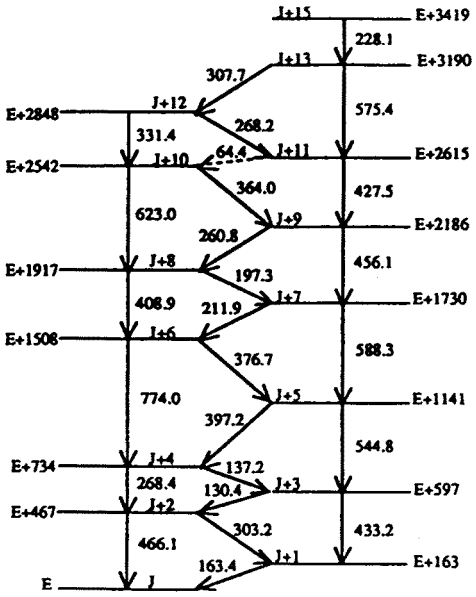

Fig. 8. Partial level scheme for the irregular band in ^{194}Pb; the level order is determined from the combination of cascade and cross-over transitions observed. Taken from Ref. [18].

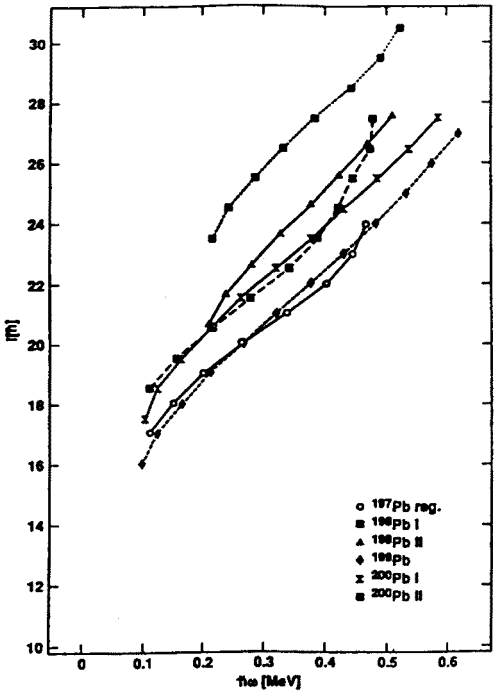

Fig. 9. Spin vs. rotational frequency for the Pb bands listed on the figure. The spins are not known for these bands; the assumed values have an uncertainty of at least ± 2ħ. Taken from Ref. [13].

the sign of the quadrupole moment (since g_K-g_R is positive for protons with j > 3/2), is negative (oblate). It appears that a similar situation occurs in the Pb bands; down-sloping high-Ω $h_{9/2}$ and $i_{13/2}$ proton levels approach the Fermi surface for moderate values (0.1) of β and for γ = -60°, and excitation into them from the upsloping $s_{1/2}$ levels becomes relatively easy. In experimental fact, isomeric states based on $\pi[(s_{1/2})^{-2}(h_{9/2})^2]_{8+}$ and on $\pi[(s_{1/2})^{-2}(h_{9/2})^1(i_{13/2})^1]_{11-}$ configurations are known in a number of the light, doubly-even Pb isotopes from mass 194 to 204. Such proton configurations provide the large magnetic moment and value of K necessary to give large B(M1) values and little signature splitting, i.e., strong coupling to the deformation axis. But neutron configurations must also be considered, especially since some of the bandheads are probably above spin = 20. Total Routhian Surface calculations [13] indicate that 2, 3, or 4 $i_{13/2}$ neutron holes also show an oblate minimum near γ = -60° at moderate rotational frequencies (0.3 MeV), although at a somewhat smaller deformation thaan the protons, β ≈ 0.06. Thus, possible configurations for the regular bands are $\pi(8^+),\nu[(fp)^{-x}(i_{13/2})^{-y}]$ and $\pi(11^-),\nu[(fp)^{-x}(i_{13/2})^{-y}]$. But in contrast to the protons which are high-Ω and strongly coupled to the nuclear symmetry axis, the $i_{13/2}$

neutron holes are low-Ω and so will align with the rotation axis already at low rotational frequencies. An indication of this alignment comes from the shape of an I vs. ω or I_x vs. ω_x plot. Figure 9 shows such a plot of I vs. ω for a number of the regular bands, and indicates an alignment of order 14-18$\hbar$ on the total angular momentum axis. This also explains the fact that the dynamic moment of inertia is only about one-third of the estimated values for the kinematic moment; the latter, I/ω, is the slope of the line from the origin to the point of the spin of interest, while the former, $dI/d\omega$, is the tangent to the plot at that point and is much the smaller of the two after a large alignment.

It is not clear at this time what differentiates the regular and irregular bands; the latter appear so far only in the lighter Pb nuclei ^{192,194,197}Pb, and so involve more neutron holes. They may have a smaller oblate deformation, that is be less collective. Or, they may have a more negative value of γ than -60° and be somewhat triaxial. It does seem necessary that they have both a high-K proton component and the aligned neutron holes characteristic of the regular bands in order to have large B(M1) values and high-spin bandheads.

The detailed structures of all these bands remains to be determined; this will necessitate the observation of the connecting transitions to the lower known states so that spins and parities and eventually configurations can be determined. As already mentioned, it has been reported that in two cases, one [20] in ^{194}Pb and one [8] in ^{199}Pb, at least some of the connecting transitions have been found. But with the new arrays coming into operation, Eurogam and Gasp in Europe and Gammasphere in the U.S., we will have much greater sensitivity to such weak lines and should be able to pick these connections out in more cases. This will lead to a better understanding of the nature of these bands, both regular and irregular. Of course, with the new arrays we will have much else to study also: superdeformation, hyperdeformation, high-spin octupole bands including the banana shapes, possible appearance of collectivity in high-spin bands above particle-hole states in near-spherical nuclei, and much more. It is an exciting time in nuclear structure work.

References:

[1] E.F.Moore et al., Phys. Rev. Lett. **63**, 360 (1989)
[2] D. Ye et al., Phys. Rev. **C 41**, R13 (1990)
[3] J. A. Becker et al., Phys. Rev. **C 41**, R9 (1990)
[4] S. Frauendorf, F. R. May, and U. V. Paskevich, *Future Directions in Studies of Nuclei far from Stability*, eds. J. H. Hamilton, E. H. Spejewski, C. R. Bingham, and E.F.Zganjar (North-Holland, Amsterdam, 1980) p. 133
[5] P. Van Duppen et al., Phys. Rev. Lett. **52**, 1974 (1984)
[6] R. Bengtsson and W. Z. Nazarewicz, Z. Phys. **334**, 269 (1989)
[7] G. Baldsiefen et al., Phys. Lett. **B 275**, 252 (1992)
[8] H. Hübel, private comunication, (1992)
[9] G. Baldsiefen et al., Z. Phys. **A 343**, 245 (1992)
[10] R. M. Clark et al., Phys. Lett. **B 275**, 247 (1992)
[11] R. M. Clark et al., Z. Phys. **A 342**, 371 (1992)
[12] T.F. Wang et al., Phys. Rev. Lett. **69**, 1737 (1992)
[13] A. Kuhnert et al., Phys. Rev. **C 46**, 133 (1992)
[14] DSAMFT_OR, from the original code by J. C. Bacelar, modified by J. Gascon and later by J. C. Wells

[15] J. F. Ziegler et al., *The Stopping and Range of Ions in Solids, Vol. I* (Pergammon Press, New York, 1985)
[16] P. M. Endt, At. Data Nucl. Data Tables **26**,47 (1981)
[17] F. Donau and S. Frauendorf, *Proc. of the Conf. on High Angular Momentum Properties of Nuclei*, ed. N.R. Johnson (Harwood Academic Press, New York, 1983) p. 143
[18] M. J. Brinkman, PhD dissertation, Rutgers University, 1991; M. J. Brinkman et al., (unpublished)
[19] B. Fant et al., J. Phys. G **17**, 319 (1991)
[20] F. Hannachi, private communication, (1992)
[21] D. B. Fossan et al., Nucl. Phys. **A520**, 241c (1990)

Acknowledgments: I would like to thank all my colleagues who have taken part in the experiments at the 88-Inch Cyclotron and who have discussed their work with me. This includes M. A. Deleplanque, J. R. B. Oliveira, W. Korten, A. O. Macchiavelli, and F. S. Stephens from Lawrence Berkeley Laboratory, J. A. Becker, E. A. Henry, A. Kuhnert, N. Roy, M. A. Stoyer, and T. F. Wang from Lawrence Livermore National Laboratory, M. J. Brinkman and J. A. Cizewski from Rutgers University, J. E. Draper and E. Rubel from University of California, Davis, W. H. Kelly and D. T. Vo from Iowa State University, S.W.Yates from the University of Kentucky, J. Burde from the Hebrew University, Jerusalem, and F. Azaiez from IPN, Orsay, France. I also thank H. Hübel from the University of Bonn and F. Hannachi from CSNSM, Orsay, France for communicating to me the information on the connecting transitions in ^{199}Pb and ^{194}Pb, respectively.